PHYSICAL REVIEW B **75**, 060101(R) (2007)

Polar and magnetic properties of $PbVO_3$ thin films

Amit Kumar,[1] Lane W. Martin,[2,3] Sava Denev,[1] Jeffery B. Kortright,[3] Y. Suzuki,[2,3] R. Ramesh,[2,3] and Venkatraman Gopalan[1]
[1]*Department of Materials Science and Engineering, Pennsylvania State University, MRL Building, University Park, Pennsylvania 16802, USA*
[2]*Department of Materials Science and Engineering, University of California, Berkeley, Hearst Mining Building, Berkeley, California 94720, USA*
[3]*Lawrence Berkeley National Laboratory, Materials Science Division, Berkeley, California 94720, USA*
(Received 24 October 2006; revised manuscript received 18 January 2007; published 8 February 2007)

Multifunctional materials promise to provide the foundation for a class of devices in which electrical, magnetic, elastic, and other properties are coupled to one another. Here we present evidence for piezoelectricity and antiferromagnetic ordering in a multifunctional material $PbVO_3$. Through the use of second-harmonic generation and x-ray linear dichroism, we determine a transition from a polar-only 4*mm* state to a polar and magnetic state below ~100–130 K. In combination with theory, the magnetic symmetry has been narrowed to be *G* type ($4'/m'mm'$) or spin glass. An effective piezoelectric coefficient of $d_{33} \sim 3.1$ pC/N was also measured in the polar state at room temperature.

DOI: 10.1103/PhysRevB.75.060101 PACS number(s): 77.84.Dy, 77.80.Bh, 42.70.Mp

Multiferroic materials, in which ferromagnetism and ferroelectricity coexist, have been of particular interest recently.[1–4] Single-phase multiferroism has been identified in only a few perovskite (ABO_3) oxides including $BiMnO_3$ (Ref. 5) and $BiFeO_3$ (Ref. 6). Here we examine a candidate multiferroic, lead vanadate—$PbVO_3$ (PVO).[7,8] It has been proposed to have antiferromagnetic ordering and a ferroelectric polarization as large as 152 $\mu C/cm^2$ due to large structural distortions in the material.[7–10]

Previous synthesis studies of PVO[7,8] focused on high-temperature and high-pressure single-crystal growth techniques. Attempts to measure the ferroelectric and magnetic properties of PVO, however, have been limited by the material itself. Shpanchenko *et al.*[7] completed a neutron diffraction study to probe the magnetic order in PVO single crystals and found neither extra antiferromagnetic peaks nor an increase in the nuclear Bragg peaks even at temperatures as low as 1.5 K. Susceptibility measurements were further limited by the inclusion of ferromagnetic impurities.[7] Recent theoretical treatments suggest a strong competition between *C*- and *G*-type antiferromagnetic order may exist in PVO. This competition could cause the formation of a complex magnetic ground state, such as a spin glass. Researchers also predict that the possible ordering temperature could be around 100–120 K based on theoretical calculations[9,10] and an observed discontinuity in resistivity data for bulk PVO near this temperature range.[7] Furthermore, Belik *et al.* attempted to measure the ferroelectric properties of this material, but due to the low resistivity of the PVO, they were unable to observe any polarization–electric-field (*P-E*) hysteresis even at liquid nitrogen temperatures. Structural studies performed at very high pressures, however, enabled Belik *et al.* to observe a tetragonal-to-cubic phase transition under 2–5.9 GPa pressure at room temperature.[8] To this point, however, the true multifunctional nature of this material is unknown to researchers. Through the use of nonequilibrium thin-film deposition techniques, we have been able to stabilize PVO on a number of single-crystal substrates, study the crystal structure of this phase, and probe the magnetic and ferroelectric properties using optical second-harmonic generation, x-ray linear dichroism, and piezoresponse force microscopy (PFM).

Details of the growth and structure of these films have been reported elsewhere.[11] Epitaxial thin films of *c*-axis-oriented PVO were synthesized using pulsed laser deposition on a number of single-crystal substrates including $NdGaO_3$ (NGO) (110).[11] Films were fully epitaxial, both in and out of the plane. Evidence from x-ray diffraction and transmission electron microscopy (TEM) studies performed suggest that the films are relaxed on all substrates studied and hence film strain considerations are not significant in our films.[11]

Magnetization measurements using a superconducting quantum interference device (SQUID) showed no evidence for strong ferromagnetic coupling in the PVO at temperatures from 2 to 380 K. Nor was any polarization hysteresis observable due to the low resistivity of PVO. Our films exhibited room-temperature resistivities between 10 and 10 000 Ω cm which are consistent with those observed in the literature.[7,8] Therefore, second-harmonic generation (SHG), x-ray linear dichroism (XLD), and PFM were used to probe the antiferromagnetism and piezoelectricity in our films.

Optical SHG[12,13] involves the conversion of light (electric field E^{ω}) at a frequency ω into an optical signal at a frequency 2ω by a nonlinear medium, through the creation of a nonlinear polarization $P_i^{2\omega} \propto d_{ijk} E_j^{\omega} E_k^{\omega}$, where d_{ijk} represents the nonlinear optical coefficient. Recently, SHG has confirmed ferroelectricity in $BiMnO_3$,[14,15] which has similarly low resisitivity. PVO films with thickness between 100 and 150 nm grown on $NdGaO_3$(110) substrates were used for this study, since $NdGaO_3$ is centrosymmetric (point group *mmm*) and does not contribute SHG signals of its own. The SHG experiment was performed with a fundamental wave generated from a tunable Ti-sapphire laser with 65-fs pulses of wavelength 800 nm incident from the film side at an angle $\varphi_i^{\omega} = 26°$ to the sample surface normal. Let us define $x = (100)_p$ and $y = (010)_p$ as the pseudocubic directions of the NGO substrate and $y = s$ as the axis normal to the incidence

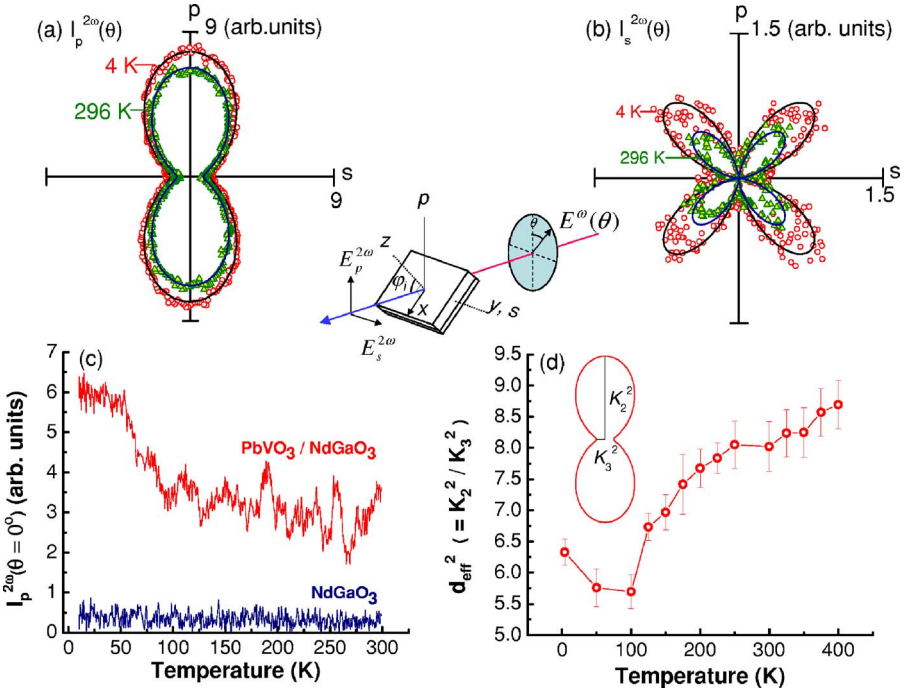

FIG. 1. (Color online) SHG of PVO films on NGO (110) substrates. Shows SHG as a function of incoming light angle for a detector fixed at (a) *p* polarization and (b) *s* polarization. (c) Shows the variation of SHG signal, $I_p^{2\omega}(\theta=0^\circ)$, as a function of temperature. (d) Shows the dimensionless effective nonlinear coefficient graphed as a function of temperature which points to a discontinuity between 100 and 130 K.

plane of light. The polarization direction of incident light is at an angle θ from the incidence plane, which was rotated continuously using a half-wave plate (inset of Fig. 1).

The intensity $I_j^{2\omega}$ of the output SHG signal at 400 nm wavelength from the film was detected along either $j=s,p$ polarization directions as a function of polarization angle θ of incident light (inset of Fig. 1). The resulting polar plots of SHG intensity for *p* and *s*-polarized output at 4 K and 296 K are shown in Figs. 1(a) and 1(b), respectively. The expected SHG intensity expressions for *s* and *p* output polarizations in the predicted 4*mm* symmetry system of PVO[7–9] are

$$I_s^{2\omega} = K_1^2 \sin^2 2\theta,$$

$$I_p^{2\omega} = (K_2 \cos^2 \theta + K_3 \sin^2 \theta)^2, \tag{1}$$

where

$$K_1 = \sqrt{I_0} f_y f_z \tilde{f}_y^T f_{s,e} d_{15} \sin \varphi_i^{\omega}, \tag{2}$$

$$K_2 = \sqrt{I_0} f_{p,e} (\tilde{f}_x^T f_x f_z d_{15} \sin 2\varphi_i^{\omega} + \tilde{f}_z^T f_x^2 d_{31} \cos^2 \varphi_i^{\omega} + \tilde{f}_z^T f_z^T d_{33} \sin^2 \varphi_i^{\omega}), \tag{3}$$

$$K_3 = \sqrt{I_0} f_{p,e} \tilde{f}_z^T f_y^2 d_{31}. \tag{4}$$

K_1, K_2, and K_3 are coefficients that are functions of the nonlinear coefficients d_{ij}, refractive indices *n* of the film and the substrate, and incidence angle φ_i^{ω}. The terms f_x, f_y, and f_z are linear Fresnel coefficients for transmission of light with frequency ω through the *incident* air-film interface while I_0 represents the incident intensity of the input beam. The terms $f_{s,e}$ and $f_{p,e}$ are linear Fresnel coefficients for *s*- and *p*-polarized SHG signals, respectively, in transmission through the *exit* substrate-air interface. The terms $\tilde{f}_x^T$, $\tilde{f}_y^T$, and $\tilde{f}_z^T$ are the nonlinear Fresnel coefficients.[16] Theoretical fits to the experimental polar plots based on Eqs. (1) are excellent as seen from Figs. 1(a) and 1(b). In normal incidence ($\varphi_i^{\omega}=0$), the film does not generate any SHG which is in agreement with the expected 4*mm* point group symmetry of the film. These findings, which are consistent with XRD and TEM measurements, indicate that PVO has a crystallographic polar point group of 4*mm* from 400 K down to 4 K.

SHG polar plot measurements were performed as a function of temperature from 4 K to 298 K, and the results are shown in Fig. 1(c). An anomaly in intensity at ~100 K is observed indicating a possible transition. This transition is clearly revealed by plotting a dimensionless effective nonlinear coefficient $\bar{d}_{\text{eff}}=(K_2/K_3)$, as shown in Fig. 1(d). It can be written as

$$\bar{d}_{eff} = \left(\frac{I_p^{2\omega}(\theta=0^\circ)}{I_p^{2\omega}(\theta=90^\circ)} \right)^{1/2} = \frac{K_2}{K_3}. \tag{5}$$

$\bar{d}_{\text{eff}}$ depends only on the nonlinear coefficients d_{ij} of the film and the refractive indices of the film and the substrate through the linear and nonlinear Fresnel coefficients. An anomaly in $\bar{d}_{\text{eff}}$ is observed at ~100–130 K. Reflection and transmission measurements at 400 nm and 800 nm for *p* and *s* polarizations for both the film and the bare substrate were performed. No anomaly in the reflection or transmission data for the film or the substrate in the concerned temperature range was observed, thus ruling out the possibility of the anomaly being generated due to refractive index change. Hence, the anomaly in $\bar{d}_{\text{eff}}$ with temperature can therefore arise from an anomaly in the nonlinear optical coefficients d_{15}, d_{31}, or d_{33} of the film. Resistivity measurements[7] give evidence for a transition in PVO around 120 K, and first-principles theory predicts an antiferromagnetic phase transition in bulk PVO at ~100 K from a high-temperature polar

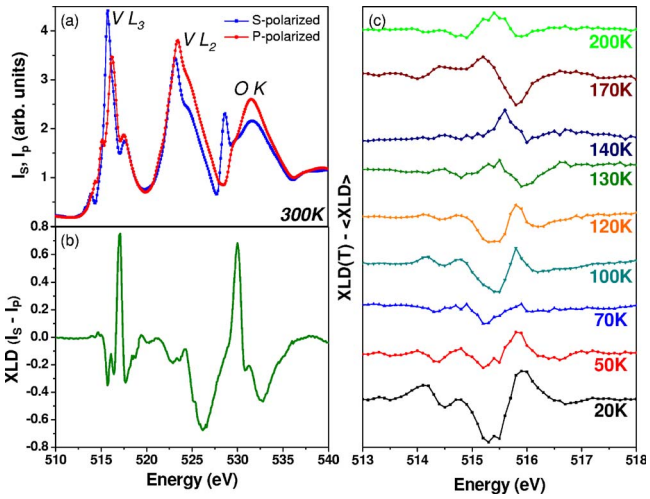

FIG. 2. (Color online) X-ray linear dichroism for PVO films on LAO (001) substrates. (a) X-ray absorption spectra for both *s*- and *p*-polarized x rays at the V and O edges in PVO. (b) Linear dichroism data for the PVO films. Shows distinct differences between the absorption of *s*- and *p*-polarized x rays. (c) Difference between the linear dichroism at a number of given temperatures and the overall average linear dichroism exhibited by PVO.

4*mm* point group symmetry to a low-temperature polar and antiferromagnetic phase of *C*-type ($4'/mmm'$) or *G*-type ($4'/m'mm'$) structure.[9,10] The observed anomaly at temperatures near that predicted in the theory could arise from the onset of antiferromagnetic order. Currently it is unclear why the anomaly observed here has not been observed in bulk samples of PVO. It is possible, as has been suggested by Singh,[10] that the nearly degenerate nature of the *C*- and *G*-type order could be creating a frustrated magnetic state in the bulk materials. Furthermore, we note that the slight structural difference between our PVO films (c=5.02 Å) and that of bulk PVO (c=4.67 Å) could result in a break in the degenerate energies for the *C*- and *G*-type ordering states and preferential selection of one over the other in our films.

To confirm the existence of a phase transition in the PVO films, we have additionally used XLD to investigate temperature-dependent changes in structural and magnetic order. XLD measures the difference in absorption of linear *s*- and *p*-polarized x rays, arising from (i) any reduction from cubic symmetry, such as the tetragonal distortion associated with ferroelectricity in PVO, or (ii) antiferromagnetic[17–20] or ferromagnetic[21] order, due to the anisotropic distribution of spin-polarized electrons relative to the magnetic axis. Spectral XLD measurements of the V $L_{2,3}$ and O *K* edges provide a highly sensitive measure of anisotropy because of the resonant dipole coupling to empty V *d* and O *p* Fermi-edge states. We measured XLD from 20 to 370 K using elastically scattered x-ray channels across the V and O edges from a (001)-oriented sample with *s*- and *p*-polarized x rays incident at 8° from grazing incidence. The *s*-polarized resonant scattering probes the electronic structure in the *a*-*b* plane and *p*-polarized scattering probes the tetragonal *c* and *a* axes.

Strong linear dichroism (LD) in scattering is evident in the scattering of *s*- and *p*-polarized x rays at 300 K in Fig. 2(a). Strong multiplet splitting is observed at the V L_3 edge (~515 eV) and to a lesser extent at the L_2 edge (~522 eV). Strong resonant features are also observed at the O *K* edge (~528 eV and above). Strong electronic anisotropy is evident in the I_s and I_p channels, in which polarization is normal to and has a component along the tetragonal axis, respectively. The linear dichroism I_s-I_p in Fig. 2(b), together with the individual curves, indicates very different populations of *d* and *p* states at the V and O sites, respectively.

We observe a strong XLD to persist over the entire temperature range, as well as a small but distinct change in XLD with temperature between 100 and 130 K consistent with a change in magnetic or structural order parameter in this range. Temperature-dependent changes in XLD are most easily observed as deviations from the temperature-averaged XLD [XLD(T)-⟨XLD⟩], where ⟨···⟩ is the temperature average of all data. The temperature average ⟨LD⟩ is from data collected at 20, 50, 70, 90, 100, 110, 120, 130, 140, 150, 160, 170, 180, 190, 200, 220, and 260 K. The mean and median values of these temperatures are 139 and 140 K, respectively, with a span of ±120 K. Thus data above and below the nominal transition are weighted roughly equally, and the trends in XLD-⟨XLD⟩ over this range do reflect an abrupt change in spectral shape. Figure 2(c) shows that at 120 K and below, we observe one characteristic shape, while at 130 K and above the characteristic shape changes sign, indicating that a transition in electronic structure has occurred between 100 and 130 K. The maximum temperature-dependent change in the XLD signal is ~6% at 515.3 eV and ~2% at 528.0 eV. The shape difference between high- and low-*T* spectra has features suggestive of an energy shift of the XLD spectrum, but is not consistent with a simple rigid energy shift. Careful examination of the data shows that the shape difference results from subtle shifts of specific L_3 multiplets relative to others. The origin of this transition at ~130 K is not uniquely identified by these spectral changes in electronic anisotropy; spin ordering into an antiferromagnetic order could cause these changes, as could a subtle change in structure and/or polarization at this temperature.

Note that both SHG (optical) and XLD (x-ray) are a measure of birefringence in electronic polarizability, albeit at very different frequencies. Confident that there is a transition occurring near ~100–130 K, we can now perform a magnetic symmetry analysis assuming that this transition is magnetic. Since the observed SHG polar plot symmetries do not change from 4 to 400 K, we can deduce the following.

(a) If the magnetic sublattice below 100 K contributes to the SHG signal, then it should have the same tensor symmetry as the polar 4*mm* point group above the transition. From this argument, point groups 4, $\bar{4}$, $4/m$, 422, 4*mm*, 2*m*, $4/mmm$, $4'22$, $4'mm'$, $\bar{4}'2m'$, $\bar{4}'2'm$, and $4'/mmm'$ are all ruled out, because of different or additional symmetries to what is observed experimentally. This argument therefore rules out the *C*-type ($4'/mmm'$) magnetic symmetry. The only third-rank axial tensors with tetragonal symmetry that are identical to the polar 4*mm* tensor are $42'2'$, $4m'm'$, $\bar{4}2'm'$, and $4/mm'm'$.

(b) If the magnetic sublattice *does not* give rise to any SHG signal below 100 K, then the observed anomaly is only due to anomalies in the polar tensor coefficients at the tran-

sition. This limits the selection to the following tetragonal magnetic point groups: $4/m'$, $4'/m'$, $4/m'm'm'$, $4/m'mm$, and $4'/m'mm'$. Thus, *G*-type ($4'/m'mm'$) is a distinct possible symmetry. An additional possibility is that the magnetic structure below 100 K is disordered, as in a spin glass, and gives no SHG signal. One way this could arise is through a competition between nearly degenerate *C*-type and *G*-type magnetic phases.[10]

The conclusion from the above analysis is that the *G*-type magnetic symmetry of $4'/m'mm'$ is the symmetry of the PVO film that is consistent with both the theoretical predictions[9,10] and the SHG experiments. If the possibility of competition between nearly degenerate *C*-type and *G*-type magnetic symmetries is allowed, then a spin glass is also a possibility. If the theory is wrong or inapplicable to our film system, there may be additional possibilities for magnetic symmetries per the discussion above.

Piezoresponse force microscopy was used to ascertain the polarization of the PVO film grown on NGO substrate. The bottom electrode was applied at the bottom of the substrate (0.5 mm thick). However, the electric field and the measured PFM displacement is almost confined entirely within ~100 nm depth under the tip and yields correct values of piezoelectric coefficient in a reference single-crystal $LiNbO_3$ sample.[22] The NGO substrate was first tested for piezoresponse, but no signal was obtained, thus ensuring that the PFM signal has contribution from the film only. Nonlocal electrostatic contributions were also eliminated by scanning nonpiezoelectric samples (such as a sample of fused silica glass) under the same tip and sample geometry. The PFM signal from the film was quite strong with good signal-to-noise ratio, which was then calibrated with a $LiNbO_3$ sample to obtain an effective piezoelectric d_{33} strain coefficient of 3.1 ± 1.5 pC/N for the PVO film. The PFM images reveal no domain structure, indicating a self-poled film.

Thus, all indications are that this material is certainly polar and piezoelectric, and is likely to be ferroelectric. However, the extreme tetragonal distortion and formation of vanadium-square pyramidal structures with shorted vanadyl bonds between vanadium and the apical oxygen may be limiting the ferroelectric switchability of PVO. Upon heating, the polar $4mm$ symmetry continues until the material decomposes at ~573 K into other phases; hence, the possible ferroelectric transition could not be probed directly. Nonetheless, PVO is truly a new multifunctional material with the simultaneous presence of piezoelectricity and magnetic order below ~130 K.

This work has been supported by the Department of Energy through a Lawrence Berkeley National Laboratory LDRD grant. We would like to acknowledge support from NSF under Grants Nos. DMR-0122638, DMR-0507146, DMR-0512165, DMR-0349632, and DMR-0213623. L.W.M. grew the thin films and performed the XLD data analysis. A.K. performed the SHG experiments and the symmetry analysis.

[1] N. A. Hill, J. Phys. Chem. B **104**, 6694 (2000).
[2] N. A. Hill and A. Filippetti, J. Magn. Magn. Mater. **242**, 976 (2002).
[3] M. Fiebig, J. Phys. D **38**, R123 (2005).
[4] N. A. Spaldin and M. Fiebig, Science **309**, 391 (2005).
[5] A. M. dos Santos, S. Parashar, A. R. Raju, Y. S. Zhao, A. K. Cheetham, and C. N. R. Rao, Solid State Commun. **122**, 49–52 (2002).
[6] J. Wang, J. B. Neaton, H. Zheng, V. Nagarajan, S. B. Ogale, B. Liu, D. Viehland, V. Vaithyanathan, D. G. Schlom, U. V. Waghmare, N. A. Spaldin, K. M. Rabe, M. Wuttig, and R. Ramesh, Science **299**, 1719 (2003).
[7] R. V. Shpanchenko, V. V. Chernaya, A. A. Tsirlin, P. S. Chizhov, D. E. Sklovsky, E. V. Antipov, E. P. Khlybovv, V. Pomjakushin, A. M. Balagurov, J. E. Medvedeva, E. E. Kaul, and C. Geibel, Chem. Mater. **16**, 3267 (2004).
[8] A. A. Belik, M. Azuma, T. Saito, Y. Shimakawa, and M. Takano, Chem. Mater. **17**, 269 (2005).
[9] Y. Uratani, T. Shishidou, F. Ishii, and T. Oguchi, Jpn. J. Appl. Phys., Part 1 **44**, 7130 (2005).
[10] D. J. Singh, Phys. Rev. B **73**, 094102 (2006).
[11] L. W. Martin, Q. Zhan, M. Chi, T. Mizoguchi, J. Kreisel, N. Browning, Y. Suzuki, and R. Ramesh, Appl. Phys. Lett. **90**, 062903 (2007).
[12] A. Kirilyuk, J. Phys. D **35**, R189 (2002).
[13] M. Fiebig, V. V. Pavlov, and R. V. Pisarev, J. Opt. Soc. Am. B **22**, 96 (2005).
[14] A. Sharan, I. An, C. Chen, R. W. Collins, J. Lettieri, Y. Jia, D. G. Schlom, and V. Gopalan, Appl. Phys. Lett. **83**, 5169 (2003).
[15] A. Sharan, J. Lettieri, Y. Jia, W. Tian, X. Pan, D. G. Schlom, and V. Gopalan, Phys. Rev. B **69**, 214109 (2004).
[16] B. Dick, A. Gierulski, G. Marowsky, and G. A. Reider, Appl. Phys. B: Photophys. Laser Chem. **38**, 107 (1985).
[17] P. Kuiper, B. G. Searle, P. Rudolf, L. H. Tjeng, and C. T. Chen, Phys. Rev. Lett. **70**, 1549 (1993).
[18] J. Lüning, F. Nolting, A. Scholl, H. Ohldag, J. W. Seo, J. Fompeyrine, J.-P. Locquet, and J. Stöhr, Phys. Rev. B **67**, 214433 (2003).
[19] A. Scholl, H. Ohldag, F. Nolting, J. Stöhr, and H. A. Padmore, Rev. Sci. Instrum. **73**, 1362 (2002).
[20] A. Scholl, J. Stöhr, J. Lüning, J. W. Seo, J. Fompeyrine, H. Siegwart, J.-P. Locquet, F. Nolting, S. Anders, E. E. Fullerton, M. R. Scheinfein, and H. A. Padmore, Science **287**, 1014 (2000).
[21] J. B. Kortright and S.-K. Kim, Phys. Rev. B **62**, 12216 (2000).
[22] D. A. Scrymgeour and V. Gopalan, Phys. Rev. B **72**, 024103 (2005).